

# Using Visible Light for Joint Communications and Vibration Sensing in Industrial IoT Applications

Muhammad Sohaib Amjad and Falko Dressler

School of Electrical Engineering and Computer Science, TU Berlin, Germany

{amjad,dressler}@ccs-labs.org

**Abstract**—The industrial Internet of Things (IoT) is becoming a core component of future industrial automation supporting smart manufacturing systems. One of the main building blocks here is the continuous health monitoring of the working machinery. Very recently, the use of strobing light in combination with cheap low-Frames Per Second (FPS) camera has been suggested as a non-invasive but very accurate measurement technology. We combine the sensing task with data communication using the same LED light sources. Indoor Visible Light Communication (VLC) is already popular as it helps reducing load on the quite crowded RF spectrum. In this work, we not only make use of the on-phase of the LEDs producing the strobing light for VLC-based data communication but also combine it with Dark Light Communication (DLC) in the off-phase. Here, only very short light pulses are used for communication, which cannot be seen by the human eye. The challenge was to maintain a constant energy envelope of the light signal for the camera-based frequency detector. We present now a fully-featured Visible Light Communication and Sensing (VLCS) system for application, e.g., in industrial environments.

## I. INTRODUCTION

Over the last years, Internet of Things (IoT) technologies have evolved significantly and have reshaped many working fields in our society through the realization of smart grids, smart manufacturing, and smart cities [1]. In particular, the integration of Cyber-Physical Systems (CPS) for smart manufacturing in industrial automation has transformed the production mode from digital to intelligent. Industrial IoT networks aim to connect almost everything in the automation process. As a result, the network is expected to have ubiquitous coverage connecting an increasing number of devices per unit area leading to a substantial aggregated bandwidth. Conventional communication in the highly exhausted radio frequency spectrum often experiences severe channel degradation and electromagnetic interference in radio-hostile industrial environments [2], [3]. This impedes the optimal performance of industrial IoT networks, which can potentially cause significant reduction in manufacturing productivity or even physical and economical damages [3].

With the recent advances in Light Emitting Diodes (LEDs) technology and its widespread adaptation for illumination, indoor Visible Light Communication (VLC) has been materialized as an access technology, which can be integrated with IoT for novel networking solutions [4]. The proliferating LED usage can offer high-density wireless *downlink links* for a large number of IoT elements that can reduce the traffic on the RF communication spectrum [5]. Additionally, VLC

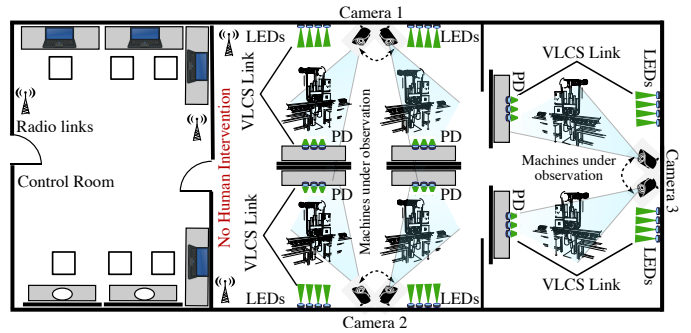


Figure 1. Joint Visible Light Communication and Sensing (VLCS) systems in radio-hostile / high-risk environment for smart industrial IoT, where each low-FPS camera is utilized for sensing vibration measurements of multiple machines.

can improve the communication reliability by complementing RF-based communication systems in radio-hostile industrial environments.

From the perspective of smart industries, continuous monitoring of machines for safety and control reasons has always been a major concern and gained significant attention in fully-automated environments. In this regards, the visible light can also be used for sensing applications in smart industries in addition to its predominant utilization for communication purposes. Roy et al. [6], [7] recently proposed a vision-based approach that uses a strobing light signal for the estimation of an object's vibration frequency. The approach utilizes a cheap commodity low-FPS camera in combination with a strobing light source for a precise approximation of the vibration frequency. The analysis of machine vibrations in an industrial environment (illustrated in Figure 1) can essentially be used as the first indicator of potential breakdowns/failures, and helps identifying the machine's health status. Additionally, it can also be utilized for the continuous optimization of the operating parameters for optimal production throughput.

For effective Visible Light Sensing (VLS), a steady envelope of the strobing light source is required. In our previous work [8], we proposed a joint VLCS system, where BPSK modulated data is communicated in the active part (*ON-Time*) of the strobing light. In this paper, we further consider Dark Light Communication (DLC), also referred to as darkVLC, to fully exploit the same LEDs for communications, even during the *OFF-Time* of the strobing light. The high switching frequency of the LEDs allows DLC [9], which operates at very high sample rates – without relying on a continuous

light source – and which is invisible to human eye. DLC is essentially filtered out by the low-FPS camera performing the sensing task. This provides the fundamental basis for using darkVLC in VLCS system. Using both the ON- and OFF-time substantially improves the communication throughput and makes the system viable for industrial IoT applications.

Our main contributions can be summarized as follows:

- We evaluate the VLCS system as a potential candidate for industrial IoT applications, performing communications and vibrations sensing for structural health monitoring.
- We use darkVLC to further improve the communication throughput and, at the same time, investigate its impact on the frequency sensing capacity of the VLCS system.
- We compare the joint VLCS system with the individual VLC and VLS systems and show that, although there is a slight performance degradation in the VLCS system, the potential gains outweigh these small losses.

## II. RELATED WORK

The incorporation of IoT in CPS-based smart grids, industrial controls and automation, medical monitoring, smart robotics, can play a pivotal role in automation and, therefore, the industrial IoT has gained much attention recently. The emerging Visible Light Communication technology with wide available spectrum in the visible light promises to overcome limiting RF resources in the densely populated radio spectrum due to huge aggregated bandwidth of the connected devices.

In this regard, the first GNU Radio-based prototype of IEEE 802.15.7 standard for short-range VLC has been introduced in [10]. In [11], an LED-based indoor broadband wireless system has been proposed achieving a data rate as high as 1 Gbit/s. Other works, such as [4], [9], have presented energy efficient variant of VLC, the darkVLC, where the data is sampled with very high sampling frequency and encoded onto very brief, imperceptible light pulses for bandwidth efficient DLC networks. In [12], [13], multiple access techniques that meet the multi-rate and delay tolerance requirements in VLC-based IoT networks have been investigated in order to address the diverse traffic characteristic in different IoT applications.

In smart industries, structural health monitoring of machines is another important aspect that has received significant attention in recent years. Here, machine vibrations are typically used as the first indicator of a possible breakdown and, thus, fault detection. Traditionally, the contact-based velocity and accelerometer sensors are usually the first choice for the measurement of vibrations. However, these sensors pose deployment and operational challenges, especially in safety-critical, high-risk, and hostile environments. Contact-less vibration sensing techniques such as Laser Doppler Vibrometer (LDV) [14] and Near-field Acoustic Holography (NAH) [15] offer precise vibration frequency estimates, but the equipment itself is rather expensive. Recently, vision-based vibration approximation, which performs image processing on a series of frames captured through a camera, has emerged as an attractive at-a-distance measuring alternative [6], [16], [17]. These contact-less approaches sometimes exploit optical strobing,

i.e., periodic light pulses [6], to obtain compelling vibration frequency estimates using cheap low-FPS cameras, making the process inexpensive and accurate.

This work incorporates the Dark Light Communication to our previous VLCS system [8], specifically for industrial IoT applications. With a substantially improved throughput level, the system can complement the existing RF communication by offloading part of the communications to the visible light spectrum, and further supports health monitoring of machines for improved safety, productivity, and cost.

## III. STROBING LIGHT-BASED VIBRATION SENSING

Strobing light is a low frequency periodic light source and it is used for recurring illumination. When a vibrating object/machine is illuminated with such a strobing light source and monitored continuously, it manifests contrasting visual presentation of its motion, i.e., from the viewers perspective the optical appearance of the object changes over time. If this monitoring is done by a camera, then the obtained frames can be analyzed by means of image processing tools to draw the temporal changes in speed of the object due to some unknown vibrational motion. The object's quantified temporal speed and position can then be capitalized for a precise estimation of this unknown vibrational frequency unobtrusively. This non-invasive approximation of vibrations (in particular of machines) can be utilized for early identification of potential faults and failures, which is important in automated and hostile industrial environments requiring least human intervention.

### A. Concept

The strobing light essentially samples an object under observation optically, and can be mathematically expressed as

$$m_s(t) = m(t) \times p(t), \quad (1)$$

where  $m(t)$  is the object with unknown vibrational frequency,  $p(t)$  is the periodic strobing light pulses, i.e.,  $p(t) = \sum_{n=-\infty}^{\infty} \delta(t - nT_s)$ , of predefined initial period  $T_s$ , and  $m_s(t)$  is the sampled object. In Fourier domain, Equation (1) can be written as

$$M_s(\omega) = \frac{1}{2\pi} [M(\omega) \otimes \frac{2\pi}{T_s} \sum_{k=-\infty}^{\infty} \delta(\omega - k\omega_s)], \quad (2)$$

where  $\omega_s$  is the strobing light frequency. The sampled signal  $M_s(\omega)$  for VLS is obtained as

$$M_s(\omega)_{VLS} = \frac{1}{T_s} \sum_{k=-\infty}^{\infty} M(\omega - k\omega_s). \quad (3)$$

This optically sampled object can be observed by a cheap low-FPS camera, which essentially has a low-pass behavior limited by the frame rate  $\omega_{cam}$ . Here, the Nyquist criterion for aliasing-free sampling certainly bounds the perceivable vibrational frequency within  $\omega_{cam}$ . Nevertheless, we can take advantage of the fact that the vibrational frequency of a typical fault-free machine is periodic in nature. Therefore, we intentionally alias the signals and the frequency folding

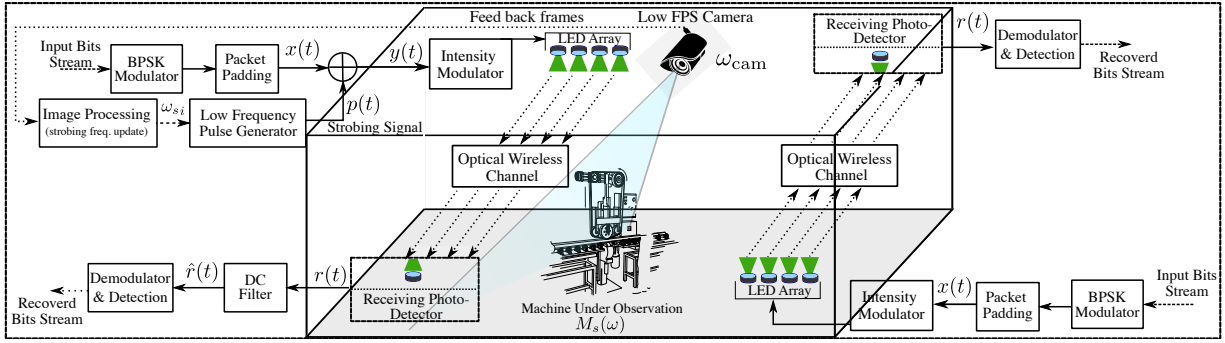


Figure 2. Detailed model of both VLCS and VLC systems for the down-link and up-link communications in an industrial environment, respectively.

phenomenon, in consequence, translates the sampled periodic spectrum in the span of  $\omega_{cam}$ , as further explained in [6], [8].

#### IV. MODELING OF VLCS SYSTEM

In our previous work [8], we modeled the integrated VLCS system, where the communication signal is sent only on the active part (*ON-Time*) of the strobing light pulses. In this work, we extend the previous model and evaluate the use of Dark Light Communication (DLC) for the joint VLCS system as well. Figure 2 presents a detailed model of both VLCS and simple VLC systems in an industrial environment. The simple VLC system is used for the up-link communications, whereas, the VLCS system is utilized for both down-link communications and non-invasive vibration sensing of machines.

##### A. Communication Model

For the down-link communication, i.e., VLCS system, (cf. Figure 2), the padded differentially BPSK modulated bit-stream  $x(t)$ , is added with the sensing (strobing) signal pulse  $p(t)$ , where the resultant signal  $y(t)$  can be defined as

$$y(t) = x(t) + p(t). \quad (4)$$

For optical transmission, the combined signal  $y(t)$  is then intensity-modulated onto an array of LEDs, and sent over the optical channel. It is worth mentioning that, unlike in previous work [8],  $x(t)$  is now independent of  $p(t)$  and the overall communication also incorporates darkVLC, i.e., communication with no reliance on a continuous light source and invisible to the human eye.

The down-link receiver is a Photo-Detector (PD) device, which converts the light intensity into an electrical signal  $r(t)$ , and can be mathematically represented as

$$r(t) = \alpha(x(t) + p(t)) + n(t), \quad (5)$$

where  $\alpha$  is the attenuation coefficient due to optical channel propagation losses and  $n(t)$  is the Additive White Gaussian Noise (AWGN) with zero mean. Since part of the communication signal  $x(t)$  is shifted up to the DC level of the strobing signal  $p(t)$ , a DC filter  $h(t)$  is used to eliminate this offset. The resultant signal  $\hat{r}(t)$  can then be expressed as

$$\hat{r}(t) = h(t) \otimes (\alpha x(t) + \alpha c(t) + n(t)). \quad (6)$$

The small ripple effect as a result of DC filtering generates residual noise  $n_{dc}(t)$  and slight distortion in  $x(t)$ , reducing Equation (6) to

$$\hat{r}(t) = \alpha \hat{x}(t) + n_{dc}(t) + n(t). \quad (7)$$

Here, we assumed  $\hat{x}(t) \approx x(t)$ , i.e., slightly distorted. The filtered received signal  $\hat{r}(t)$  is then demodulated and decoded to recover the original bit-stream. Note that, in the case of up-link VLC system, there is no sensing signal, i.e.,  $n_{dc}(t) = 0$ .

From Equation (7), the instantaneous Signal-to-Noise Ratios (SNRs)  $\gamma_{VLCS}$  and  $\gamma_{VLC}$  for both down-link and up-link communications can be computed as

$$\gamma_{VLCS} = \frac{\alpha^2 \cdot P_s}{\sigma^2 + \sigma_{dc}^2}, \quad \text{and} \quad \gamma_{VLC} = \frac{\alpha^2 \cdot P_s}{\sigma^2}, \quad (8)$$

where  $E\{|x(t)|^2\} \approx E\{|\hat{x}(t)|^2\} = P_s$  is the instantaneous signal power,  $E\{|n_{dc}(t)|^2\} = \sigma_{dc}^2$  is the DC filtering noise, and  $E\{|n(t)|^2\} = \sigma^2$  is the AWGN power. Essentially, the SNR loss  $\Gamma_L$  in VLCS because of  $\sigma_{dc}^2$  can be presented as

$$\Gamma_L = \gamma_{VLCS}/\gamma_{VLC} = \frac{1}{1 + \sigma_{dc}^2/\sigma^2}. \quad (9)$$

In Equation (9), for very small values of  $\sigma_{dc}^2$ , the SNR loss  $\Gamma_L \approx 0$ , i.e., the communication performance of VLCS system is roughly same as VLC system.

##### B. Sensing Model

The low-FPS camera capturing the illuminated machine frame, as depicted in Figure 2, performs the sensing task in the VLCS system. The sensing model here primarily studies the impact of DLC on the strobing signal, and eventually on the non-invasive sensing task.

When darkVLC is involved in VLCS, the communication signal  $x(t)$  can be presented as the sum of  $x_{SL}(t)$  and  $x_{DL}(t)$ . The  $x_{SL}(t)$  is the part of  $x(t)$  that is communicated only on the strobing light (SL) pulse (the previous work [8]), and the  $x_{DL}(t)$  is the part of  $x(t)$  that is sent as darkVLC, i.e., communicated during the *OFF-Time* of the strobing light pulse, as illustrated in Figure 3.

The machine that is optically sampled with such a strobing light signal, can be mathematically modeled as

$$m'_s(t) = m(t) \times (x_{SL}(t) + x_{DL} + p(t)). \quad (10)$$

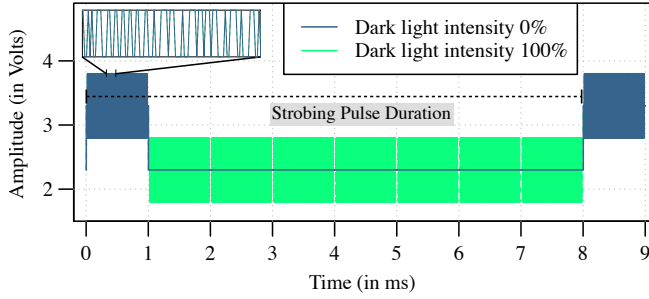


Figure 3. The strobing light signals in the VLCS system with two different DLC intensities. DLC 0% means  $x_{DL}(t) = 0$ , and DLC 100% means communications over the entire strobing pulse duration.

The Fourier domain representation is obtained as

$$M'_s(\omega) = \frac{1}{2\pi} [M(\omega) \otimes (X_{SL}(\omega) + X_{DL}(\omega)) + M(\omega) \otimes P(\omega)]. \quad (11)$$

This sampled machine  $M'_s(\omega)$  is captured by a low-FPS camera with a low-pass behavior that filters out the high frequency communication signal. Using Equation (3), the optically sampled signal in VLCS system can be written as

$$M'_s(\omega)_{VLCS} = M_s(\omega)_{VLS} + N_{SL}(\omega) + N_{DL}(\omega), \quad (12)$$

where  $N_{SL}(\omega)$  and  $N_{DL}(\omega)$  are the filtered noises. It is worth noting here that when there is no darkVLC the VLCS is expected to have less noise in general, and incorporating the darkVLC can have a slight negative impact on the sensing performance of the VLCS system.

The resulting error in the optical sampling process due to the added communication signal can be computed as

$$\|e_{err}\|^2 = \|M'_s(\omega)_{VLCS} - M_s(\omega)_{VLS}\|^2 = \|N_{SL}(\omega) + N_{DL}(\omega)\|^2. \quad (13)$$

Note that when  $\{N_{SL}(\omega), N_{DL}(\omega)\} \rightarrow 0$ , the sensing performance of VLCS system approaches to a typical VLS system.

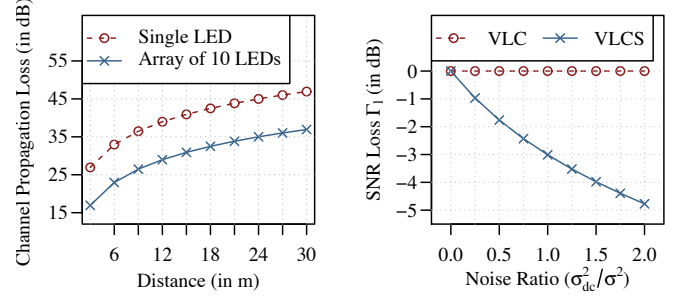
## V. PERFORMANCE EVALUATION

### A. Implementation Details

For the evaluation of our VLCS system, both the communication and sensing parts are implemented in GNU Radio.<sup>1</sup> The GNU Radio signal processing framework supports both real-time experiments and offline simulation. Our VLCS system comprises of two parts:

1) *Communications*: The system implements differential BPSK for baseband modulation/demodulation of the input bit-stream (cf. Figure 2). A packet padding block is used in the implementation to control the DLC intensity (ranging from 0%–100%) in the integrated VLCS system. The padded stream is then added with the strobing signal, which is intensity modulated (also simulated in GNU Radio) for the optical transmission.

For the optical wireless channel, we have used the same model that is presented in our previous work, for a  $10 \times 1$  LED panel and a single Photo-Detector (PD). There, the propagation



(a) Channel propagation loss in VLC. (b) Impact of increasing DC filter noise.

Figure 4. Optical propagation loss over increasing distances in the free-space for Lambertian pattern-based LEDs, and the SNR loss ( $\Gamma_l$ ) due to increasing DC filter noise.

loss  $\alpha$  is computed for LEDs following Lambertian far-field pattern defining the maximum intensity region as

$$\alpha = \frac{2D^2}{\Theta^2 d^2}, \quad (14)$$

where  $\Theta$  is the full-angle transmit beam divergence (in rad),  $d$  is the distance between the optical transmitter-receiver system, and  $D$  is the diameter of the optical receiver aperture (see [8] for more details). For a beamwidth  $\Theta = 120^\circ$ , and a PD aperture diameter of 30 cm, the free-space propagation loss over increasing distance is plotted in Figure 4a, for both a single LED and the  $10 \times 1$  LEDs panel. The same channel propagation loss values are used in the simulations for evaluation reasons.

In the VLCS system, at the receiver, a DC filter is required between the PD and the demodulation block, to filter out the strobing signal  $p(t)$ . The non-ideal design of the DC filter essentially causes ripple effect, creating some remnant noise  $\sigma_{dc}^2$  and distortion as discussed in Section IV-A. This impact of DC filter noise is also shown in Figure 4b, where clearly, the SNR loss  $\Gamma_l$  (obtained in Equation (9)) increases as soon as the DC filter noise  $\sigma_{dc}^2$  surpasses the AWGN noise  $\sigma^2$ .

2) *Sensing*: For effective sensing of vibrations, a steady envelope of the strobing signal is the foremost requirement. Especially in DLC, where the communications is performed throughout the strobing signal duration, the impact of combined signal in VLCS on the sensing is an interesting and first step to consider. For this reason, we first studied the difference in envelopes of the strobing signals in both VLCS and pure VLS systems as

$$\|E\|^2 = \|\text{Envelope} \langle y(t) \rangle - \text{Envelope} \langle p(t) \rangle\|^2. \quad (15)$$

Figure 5 demonstrates the difference between the envelopes of the VLCS and VLC strobing signals. In the plot, the mean error value is below  $-50$  dB, which is negligibly small, and shows how little is the impact of added communication signal in VLCS system on strobing pulse. This certainly ensures the capacity of joint VLCS system to effectively perform both communications and sensing. With a steady envelope in VLCS even with darkVLC, the second step extends the sensing evaluation with an emulated low FPS camera behavior within GNU Radio.

<sup>1</sup><https://www.gnuradio.org/>

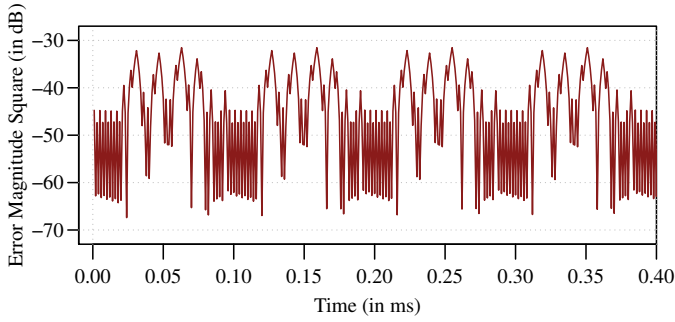


Figure 5. Error between the envelopes of VLCS and VLS strobing signals.

### B. Measurement Setup

In the setup for simulation experiments, we transmitted 1000 differentially modulated BPSK packets with different intensities of darkVLC. The considered packet structure has a 2 B preamble, 9 B of payload, and 1 B CRC. The simulations were repeated 10 times to obtain a 95 % confidence interval, and they primarily investigate the throughput performance under different DLC intensities, the achievable bit rate for the possible incorporation of the VLCS system in industrial IoT applications, and the vibration sensing capacity of the VLCS system, especially the impact of darkVLC on the strobing signal. The most relevant simulation parameters are listed in Table I.

### C. VLCS System Communication Performance

1) *Throughput Gain*: Figure 6 presents the achievable throughput levels by capitalizing different percentages of the dark light for communication purposes. The Dark Light Communication (DLC) intensity 0% means that the data is only communicated during the *ON-Time* of the strobing signal, i.e., our previous work [8], whereas the DLC 100% means that the data is communicated during the whole strobing signal duration. The resultant time domain waveforms in both cases is illustrated in Figure 3. To have a fair comparison, same transmit power is used to compute these throughput levels in both VLCS and VLC systems. Clearly, the utilization of DLC improves magnitudes of the throughput capacity as compared to the basic VLCS system previously presented with no darkVLC. Additionally, it can be seen that the throughput performance of VLCS system is relatively lower than simple

Table I  
KEY PARAMETERS OF THE JOINT VLCS SYSTEM.

Modulation	Differential BPSK
Packet Sent	1000
Bytes-per-Packet	12 B
Preamble + Payload + CRC	2 B + 9 B + 1 B
Samples-per-Packet	96
Interpolation Rate	3×
Sampling Frequency	2 MHz
Noise Floor (14-bit DAC)	-84.3 dB
Emulated Low FPS Camera Cut-off	100 Hz
Photo-Detector Aperture (D)	0.3 m
LED Array Panel	10 × 1

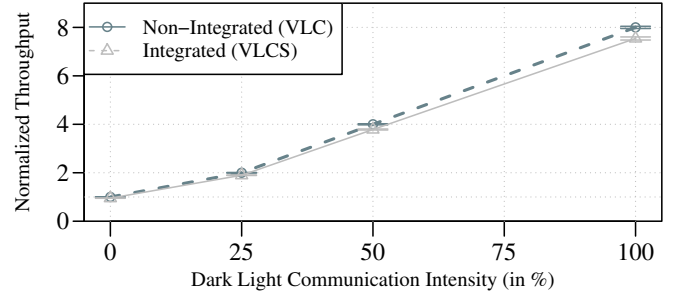


Figure 6. Achievable throughput levels with different percentages of dark light utilized for communications in joint VLCS and simple VLC systems.

VLC system for the same transmit power. This is certainly because of the additional noise and signal distortion due to the DC filtering of strobing signal, which we have discussed in the Section IV-A. Nevertheless, the gains with VLCS system to perform both communication and sensing, surely outweighs the small degradation in the performance.

2) *Achievable Data Rates*: Figure 7 presents the attainable data rates with the proposed VLCS system at various distances. The maximum achievable data rate with the current system is 640 kbit/s with 100 % dark light communication intensity. In the case, of no darkVLC, i.e., 0% DLC intensity, the maximum data rate that can be reached is 80 kbit/s. These data rates, nevertheless, are strictly bounded by the employed sampling frequency, which in the current simulation experiments is selected as 2 MHz, and they can certainly be improved by using a higher sampling frequency and efficient modulation techniques. Additionally, in the plot, it can be seen that these data rates are maintainable up-to the simulated distances of 18 m with a transmit power of 22 dBm. These measured data rates and the communication distances definitely provide valuable performance insights, and they are especially interesting if the joint VLCS system is to be considered in industrial IoT for smart automation and safety applications.

### D. VLCS System Sensing Performance

Figure 8a presents the two frequencies detected using the strobing signals of VLCS system with 100 % DLC and simple

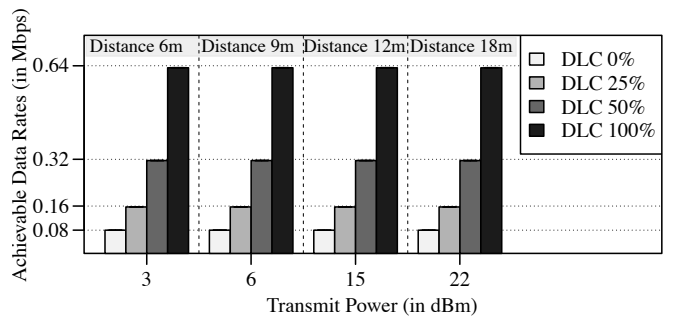
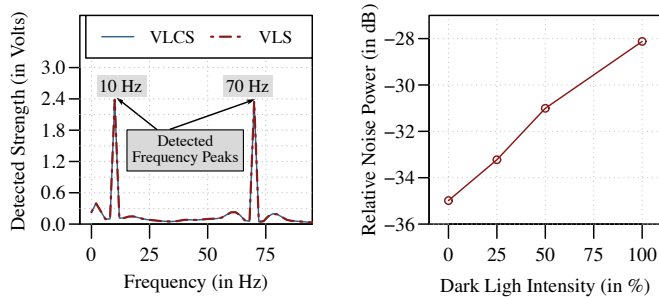


Figure 7. The measured data rates with the VLCS system utilizing different percentages of the dark light for communications at various distances. The required transmit powers correspond to the distances in order to achieve optimal data rates.



(a) Detected frequency, VLS vs. VLCS with 100% DLC.

(b) Noise power with increasing intensity of DLC.

Figure 8. The detected frequencies in VLS and VLCS emulated environments with 100% DLC, and the relative noise power with different DLC intensities.

VLS system, in the emulated environment. To understand the impact of communication signal on the sensed frequencies, we sampled two known frequencies 10 Hz and 70 Hz with both strobing signals. As can be seen in the plot, the detected frequencies are remarkably similar with both VLCS and VLS strobing signals. Such accurate frequencies detection is rather expected as we have already seen an insignificantly small error magnitude between the envelopes of two pulse in the earlier section (cf. Figure 5).

Additionally, it can be observed in Figure 8b that the noise level has jumped by 7 dB as the DLC intensity is increased from 0%–100%. This higher relative noise is anticipated at stronger DLC intensities due to the additional background noise factor  $N_{DL}(\omega)$ , as discussed in Section IV-B. These results evidently indicate that DLC have a negative impact on the sensing performance, however, it does not introduce any considerable error while detecting the frequencies, and at the same time, darkVLC supports much higher throughput, which is certainly beneficial in industrial IoT applications, connecting everything for smart automation.

At this point, it is worth mentioning that once the vibrational frequency of a machine is approximated, it remains the same unless there is a fault. Thus, the same low FPS camera can be time shared among multiple machines for sensing the vibration and logging the data. In addition to that, the same cameras can also perform security tasks effectively as well, as illustrated in Figure 1.

## VI. CONCLUSION

We introduced a complete Visible Light Communication and Sensing (VLCS) system for application in industrial environments. Here, the upcoming industrial Internet of Things (IoT) is already an integral part, however, novel communication technologies need to be investigated to overcome the limitations of the very crowded RF spectrum. Visible Light Communication (VLC) is considered a promising alternative. In this paper, we combine such an indoor VLC system with an optical sensing approach for health monitoring of machines and other industrial installations. In particular, we use a strobing light-based frequency detection, using a low-Frames Per Second (FPS) camera to determine the vibration frequency

of a machine under observation. We modulate the VLC signal in both the on-phase using classical VLC as well as in the off-phase of the strobing light, making use of the Dark Light Communication (DLC) concept. The key challenge was to maintain a constant energy envelope of the light signal for the frequency detection. We have demonstrated in this paper that the overall performance of our VLCS system is close to a VLC-only system that now integrates the sensing mechanism in the same light spectrum even with darkVLC.

## REFERENCES

- [1] L. Da Xu, W. He, and S. Li, "Internet of things in industries: A survey," *IEEE Transactions on Industrial Informatics*, vol. 10, no. 4, pp. 2233–2243, Nov. 2014.
- [2] J. Chilo, C. Karlsson, P. Angskog, and P. Stenumgaard, "EMI disruptive effect on wireless industrial communication systems in a paper plant," in *IEEE EMC 2009*, Austin, TX, Oct. 2009, pp. 221–224.
- [3] L. Wan, G. Han, L. Shu, S. Chan, and N. Feng, "PD source diagnosis and localization in industrial high-voltage insulation system via multimodal joint sparse representation," *IEEE Transactions on Industrial Electronics*, vol. 63, no. 4, pp. 2506–2516, 2016.
- [4] K. Kadam and M. R. Dhage, "Visible light communication for IoT," in *iCATect 2016*, Bengaluru, India, Jul. 2016, pp. 275–278.
- [5] D. Karunatilaka, F. Zafar, V. Kalavally, and R. Parthiban, "LED Based Indoor Visible Light Communications: State of the Art," *IEEE Communication Surveys & Tutorials*, vol. 17, no. 3, pp. 1649–1678, Mar. 2015.
- [6] D. Roy, A. Ghose, T. Chakravarty, S. Mukherjee, A. Pal, and A. Misra, "Analysing Multi-Point Multi-Frequency Machine Vibrations using Optical Sampling," in *IoPARTS 2018*, Munich, Germany, Jun. 2018, pp. 55–59.
- [7] D. Roy, S. Mukherjee, B. Bhowmik, A. Sinharay, R. Dasgupta, and A. Pal, "An autonomous, non-invasive vibration measurement system using stroboscope," in *ICST 2016*, Chinandega, Nicaragua, Nov. 2016, pp. 1–6.
- [8] M. S. Amjad and F. Dressler, "Integrated Communications and Non-Invasive Vibrations Sensing using Strobing Light," in *IEEE ICC 2020*. Virtual Conference: IEEE, Jun. 2020.
- [9] Z. Tian, K. Wright, and X. Zhou, "The DarkLight Rises: Visible Light Communication in the Dark," in *ACM MobiCom 2016*. New York City, NY: ACM, Oct. 2016.
- [10] C. G. Gavrincea, J. Baranda, and P. Henarejos, "Rapid prototyping of standard-compliant visible light communications system," *IEEE Communications Magazine*, vol. 52, no. 7, pp. 80–87, Jul. 2014.
- [11] A. M. Khalid, G. Cossu, R. Corsini, P. Choudhury, and E. Ciaramella, "1-Gb/s Transmission Over a Phosphorescent White LED by Using Rate-Adaptive Discrete Multitone Modulation," *IEEE Photonics Journal*, vol. 4, no. 5, pp. 1465–1473, Oct. 2012.
- [12] D. Chen, J. Wang, H. Lu, L. Feng, and J. Jin, "New Construction of OVSF-OZCZ Codes in Multi-Rate Quasi-Synchronous CDMA VLC Systems for IoT Applications," *IEEE Access*, vol. 8, pp. 130888–130895, Jan. 2020.
- [13] H. Yang, W.-D. Zhong, C. Chen, and A. Alphones, "Integration of Visible Light Communication and Positioning within 5G Networks for Internet of Things," *IEEE Network*, vol. 34, no. 5, pp. 134–140, Sep. 2020.
- [14] P. Castellini, M. Martarelli, and E. Tomasini, "Laser Doppler Vibrometry: Development of advanced solutions answering to technology's needs," *Elsevier, Laser Doppler Vibrometry*, pp. 1265–1285, 2006.
- [15] M. Martarelli and G. Revel, "Laser Doppler vibrometry and near-field acoustic holography: Different approaches for surface velocity distribution measurements," *Mechanical systems and signal processing*, vol. 20, no. 6, pp. 1312–1321, 2006.
- [16] K.-S. Son, H.-S. Jeon, J.-H. Park, and J. W. Park, "A technique for measuring vibration displacement using camera image," *Transactions of the Korean Society for Noise and Vibration Engineering*, vol. 23, no. 9, pp. 789–796, 2013.
- [17] J. G. Chen, N. Wadhwa, Y.-J. Cha, F. Durand, W. T. Freeman, and O. Buyukozturk, "Structural modal identification through high speed camera video: Motion magnification," in *IMAC 2012*. Brescia, Italy: Springer, Jul. 2012, pp. 191–197.